Erg-O: Ergonomic Optimization of Immersive Virtual Environments

Roberto A. Montano Murillo, Sriram Subramanian, Diego Martinez Plasencia
School of Engineering and Informatics, University of Sussex, Brighton, United Kingdom
{r.montano-murillo, sriram, d.martinez-plasencia}@sussex.ac.uk

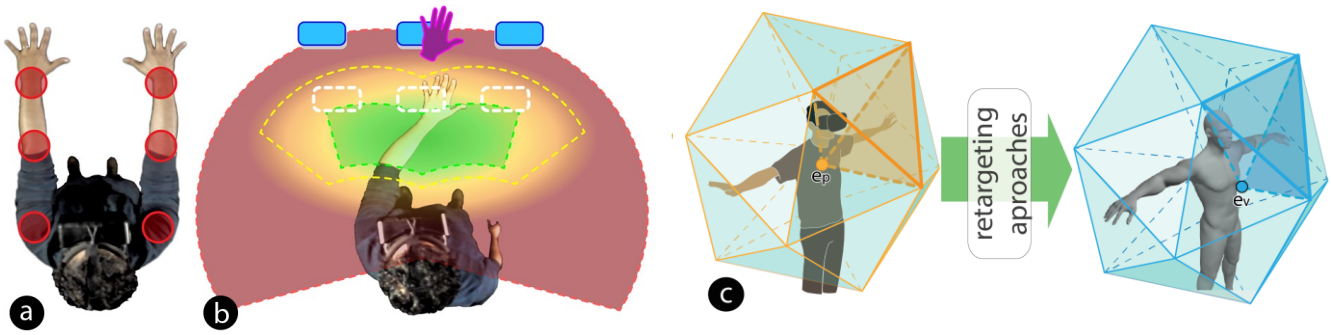

Figure 1: (a) VR involves interactions with upper limbs, which can lead to discomfort (b) Out approach retains visual objects in their location, but users can reach them from more comfortable positions (c). Our approach is based on defining two space partitioning trees, and using optimization approaches to look for most comfortable retargetings (visual to physical positions).

ABSTRACT

Interaction in VR involves large body movements, easily inducing fatigue and discomfort. We propose Erg-O, a manipulation technique that leverages visual dominance to maintain the visual location of the elements in VR, while making them accessible from more comfortable locations. Our solution works in an open-ended fashion (no prior knowledge of the object the user wants to touch), can be used with multiple objects, and still allows interaction with any other point within user's reach. We use optimization approaches to compute the best physical location to interact with each visual element, and space partitioning techniques to distort the visual and physical spaces based on those mappings and allow multi-object retargeting. In this paper we describe the Erg-O technique, propose two retargeting strategies and report the results from a user study on 3D selection under different conditions, elaborating on their potential and application to specific usage scenarios.

Author Keywords
Virtual reality; ergonomics; optimization.

ACM Classification Keywords
H.5.2. [User interfaces]: Ergonomics.

INTRODUCTION

Recent market studies foresee VR will become mainstream, reaching a $62 billion market by 2025 [34]. The rise of commercial VR devices, tracking technologies and 3D graphics have enabled increasingly compelling VR systems, not only in displaying realistic content but also allowing more natural interactions [43] and better feeling of presence [39]. Beyond entertainment, training environments can easily take advantage of this (e.g. flight or surgery simulators [40, 41]), as users are allowed to interact with the virtual environment (VE) in much the same way as they would do in reality, softening the learning process [12].

However, such natural VR interaction often involves large body motions (mainly affecting upper limbs) [46], which can result in fatigue and discomfort [23] (see Fig 1.A). This is especially true for demanding (i.e. complex or repetitive) tasks, or gaming activities for long periods.

One possible solution is to place the interactive elements (e.g. buttons, menus) at ergonomically comfortable positions, using ergonomic evaluation metrics such as RULA [32] or Jack [3]. This can be useful for in-game menus or in scenarios where the VR designer is free to pick the location of the interactive elements around the user.

Unfortunately, such ergonomic relocation might not be applicable to a pilot cockpit, or training scenarios where the virtual object resembles a real one, and interactive parts cannot be relocated. Manipulation techniques, such as Go-Go [36], might allow users to reach distant objects, while keeping arms in closer, more comfortable positions for the user (i.e. avoid overstretching of the arms). However, this technique loosens the egocentric manipulation metaphor (i.e. virtual hand), reduces precision at longer distances [22], affects the feeling of body ownership [30] and can be

undesirable for training/simulation scenarios where the user needs to be aware of the actual limits of his interaction space (i.e. what she/he will actually be able to reach/do in the real situation)[21, 37].

Our proposed solution is to get benefit of the dominance of human visual system over the proprioceptive system. We retain the visual position of the elements in the VE, but allow users to reach them from more ergonomic physical positions (Fig 1.b). This is possible as changes in position of only a few cm can increase comfort significantly.

We first contribute a manipulation technique that allows such ergonomic retargeting for a variable number of interactive elements within the user's arm reach. Our solution wraps the interactive space around the user, ensuring that: **a)** the virtual hand reaches the visual location of the interactive element, when the physical hand reaches the retargeted physical location of the element (Figure 1b); **b)** the technique works in an open ended fashion, not needing prior knowledge on the element the user wants to reach at each point; and **c)** any other point within the user's arm reach is still reachable, with continuity of interaction even when reaching between interactive elements.

We combine our manipulation technique with optimization methods, to enable online computation of optimum *retargeting mappings* (i.e. most ergonomic retargeted position to interact with the visual representation of each interactive element). We describe two example optimization strategies to obtain such mappings (*Spatial Consistent* (*S_R*) and *Ergonomic* (*E_R*)), and report the results from a user study with 12 participants, comparing *S_R* and *E_R* approaches to natural virtual hand interaction.

Our results show that participants' comfort was improved according to quantitative data (RULA score) as well as subjective judgement in retargeting conditions (*S_R* and *E_R*) compared with the natural (*N*) condition (one to one mapping without retargeting). Additionally, we found that execution time was lower in *S_R* and *E_R* conditions compared with *N* condition. These results illustrate the benefits that the multi-object retargeting enabled by ERG-O can provide for a general VR system using virtual hand interaction. We finish the paper reflecting on how the technique can also be applied for other application scenarios, such as rehabilitation or reinforcing spatial skill training for patients with cerebral palsy.

RELATED WORK

Our technique can be categorized as an egocentric virtual hand metaphor according to VR manipulation taxonomies [22]. To better appreciate our contribution, our review is focused on two main areas: (1) visual dominance and spatial redirecting; and (2) ergonomic assessment.

Visual dominance and Spatial redirecting

Visual dominance refers to the tendency of visual information to determine what is perceived when conflicting information is perceived through the visual channel and any other modality [19].

This effect has been extensively exploited in VR [14], with best known applications for navigation techniques such as redirected walking, or to avoid visual penetration of the virtual hand inside solid objects (e.g. rubber-band virtual hand [14]). However visual dominance can also influence the way in which we perceive our own body, such as having a bigger belly or even having a child's body [5, 24, 33]. When combined with synchronized multisensorial stimuli, it can even be used to induce illusions of executing actions, such as speaking [6] or walking [28].

Closer to our approach, visual dominance has also been studied in the context of hand interaction. Burns et al. [14] found very strong dominance of visual over proprioceptive perception when no tactile feedback is provided. This allowed for up to 20 cm just noticeable differences (JND) between the real and virtual hand location, before becoming noticeable (75% recognition rate), even if users were aware that a mismatch could become present.

This mismatch threshold is significantly reduced if vibrotactile cues are introduced to reinforce proprioception or when other body parts are involved. Lee et al. [29], reported JND thresholds of 5.2 cm when cutaneous haptic feedback (normal and shear forces) was applied to the fingertip. Matsuoka et al. [31] report average JND thresholds of 3.2 cm for finger flexion when force feedback is applied. Direction of forces [7] or the curvature of the physical props [38] can also influence these thresholds.

These knowledge has allowed the development of various redirection techniques for manipulation. Haptic retargeting [1] and Sparse Haptic Proxy [17] create the illusion of touching several virtual objects. Unlike Erg-O, the target of interaction must be known a priori and it only applies to stream-lined interaction (i.e. hand at a rest position, then touch the target object), not allowing free hand movements. Valkov et al. [45] proposed a technique using the display surface of a stereoscopic flat display as the passive haptic prop for shallow 3D interaction. Redirected touching [26] uses a flat board to induce the feeling of touching rotated objects. Unlike ERG-O, these techniques are usually limited to a single point of interaction (i.e. a finger) and require previous knowledge on the target of the interaction.

Leveraging thin-plate spline warping [10], approaches have been reported that allow mapping point interactions (e.g. fingers, surgery tools) to passive, non-flat surfaces of known geometry [4, 27, 42]. However, ERG-O is the first VR manipulation technique to tackle redirection for the whole interactive space around the user, not being limited to single points or surfaces and operating in an open ended fashion (i.e. target of interaction not known a priori).

Ergonomics

Ergonomic assessment has been extensively used to assess risks in workspaces, but also to evaluate interaction within HCI. These methods can be divided into: self-report, observational methods and direct measurement [13].

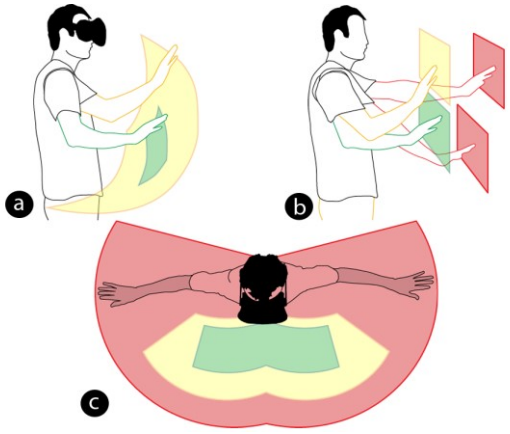

Figure 2: Comparison of different ergonomic metrics (RULA, CE). These all identify regions of space for more comfortable interaction with observable similarities.

Self-report methods (e.g. NASA-TLX [15] or the Borg CR10 scales [9]) usually involve questionnaires, ranked by using Likert-scales. These methods, however, do not allow for online assessment (while the task is carried out), and the need to rate difficultly quantifiable parameters (e.g. workload) can compromise reliability of the results [47].

Observational methods and direct measurement allow for online assessments, and the development of marker-less sensing techniques is slowly removing this distinction. Previous observational methods such as RULA [32] or Jack [3] can now be directly measured using nonintrusive wearable devices or depth cameras [35].

Other recent approaches include Consumed Endurance, which uses ergonomic models for the online assessment of mid-air planar interactive spaces [23]. Bachynskyi et al. [2] evaluated user muscle effort in 3D pointing tasks using EMG. They detect muscle activation and apply clustering techniques to identify movements with low muscle effort.

These techniques (illustrated in Figure 6), show a strong and consistent correlation between the space around the user and the most comfortable regions, with the middle area below the user's chest being consistently ranked as most comfortable. These techniques also show how a change within the JND threshold allowed by visual dominance (i.e. a few centimeters) can have important effects on ergonomic scores For instance, if our arm is fully extended aside with the hand at chest's height, moving the hand just 5cm towards the belly, will reduce the RULA score from 5 (medium-high risk) to 2 (low risk).

ERG-O builds on these observations and methods, using these areas to guide our optimization methods and finding ergonomically acceptable mappings to retarget the interactive elements of the VE and improve comfort.

ERG-O: ERGONOMIC OPTIMIZATION FOR REDIRECTED INTERACTION:

ERG-O allows redirected interaction with the interactive elements of the VE. Leveraging visual dominance and ergonomic criteria, we reposition the physical location of the interactive elements (e.g. buttons on a cockpit), but we maintain their visual location. Besides reaching these elements from more ergonomic positions, users can still interact/reach any other point of the 3D space around them. Thus, ERG-O is the first manipulation technique to allow:

- Open-ended, Multi-object retargeting (i.e. ERG-O can retarget several objects, with free hand movement and not knowing which object the user intends to reach).
- Isomorphic visual-to-physical mapping (i.e. only the visual points a user would be able to reach in reality are accessible. Each point of the visual space is mapped to one (and only one) point in physical space.
- Optimization-based computation of retargeting mapping (i.e. automatic computation of the physical location that leads to most ergonomic interaction, while minimizing visual-to-physical mismatch).

In order to realize these features, our approach is decomposed in two main stages:

First, we create a *multi-object retargeting technique*. We partition the user's reachable space into tetrahedrons, with their vertices either on the boundary (limit of user's arm reach) or on a retargeted point. Each tetrahedron describes a volume in the visual space (**V**) and its matching volume in physical/retargeted space (**P**). However, their shapes will differ slightly, as a vertex on a retargeted point will have different coordinates in **V** and **P**.

This topology of matching tetrahedrons is key to Erg-O. When the (physical) hand is anywhere inside a physical tetrahedron, the virtual hand can be mapped to a equivalent point in the matching visual tetrahedron. When a physical hand reaches a vertex, the virtual hand is mapped to the equivalent vertex, whether this is a retargeted point (this allows our multi-object retargeting); or a boundary point (this still allows users to reach the extents of their natural interactive area). As the mapping only depends on the hand location, hands can be moved freely (open-ended).

At the second stage, we compute the *retargeting mapping*. This determines the best physical location to reach each visual element, using ergonomic and spatial criteria. Our technique dynamically adapts to the current interactive elements within user's reach (i.e. their number and position relative to the users will change as they move in the VE). We describe two example approaches to compute such *retargeting mappings*, one focused on maintaining the structural relationship between the interactive elements and a second one focused on improving ergonomic interaction.

These two stages are formally described in the following two subsections. For these explanations, we will make use of right hand systems of reference, homogeneous coordinates (i.e. 3D points in A's coordinates as $\boldsymbol{p_A}(x, y, z, 1) \in \mathbb{R}^4$) and homogeneous transformation matrices ($\boldsymbol{\mathcal{M}_B^A} \in \mathbb{R}^{4x4}$, to convert coordinates from A to B).

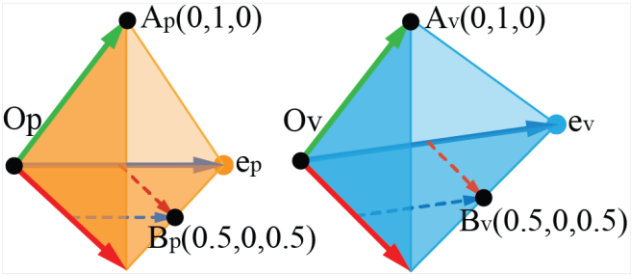

Figure 3: Example of a tetrahedron pair, defining a volume in space P and its equivalent (slightly different) volume in V. Vertex *O* and edges are used to define their local systems of reference. This allows mappings any point in tetrahedron P to a single point in tetrahedron V, enabling retargeting.

Retargeted manipulation: Bijective mapping of Visual and Physical spaces

Virtual hand interaction in VR usually assumes a direct correspondence between the physical space (**P**), around the user; and the virtual space (**V**), around its avatar. All points are mapped from one space to another directly through a transformation matrix (e.g. $\boldsymbol{p_V} = \boldsymbol{\mathcal{M}_V^P} \cdot \boldsymbol{p_P}$).

Our multi-object retargeting requires a more complex mapping, at least for the points in space within user's reach. As introduced earlier, we use tetrahedrons as the basic space partitioning unit, and build two equivalent space partitioning trees (same structure), one for each space **P** and **V**. The steps required are detailed in the next subsections.

Tetrahedrons as basic space partitioning units:

Our approach uses a set of tetrahedrons pairs (see Figure 3), one defined in each space, **P** and **V**. Let $\boldsymbol{T_V} = \{\boldsymbol{a_V}, \boldsymbol{b_V}, \boldsymbol{c_V}, \boldsymbol{d_V}\} \subseteq \boldsymbol{V}$ and $\boldsymbol{T_P} = \{\boldsymbol{a_P}, \boldsymbol{b_P}, \boldsymbol{c_P}, \boldsymbol{d_P}\} \subseteq \boldsymbol{P}$ be a tetrahedron pair described by the visual coordinates and retargeted physical coordinates, relative to user's torso (**T**).

For each tetrahedron, it is possible to describe its own non-orthogonal and non-homogeneous system of reference, using their three edges and its first vertex as column vectors (matrix $\boldsymbol{\mathcal{M}_V^T}$ can be computed analogously):

$$\boldsymbol{\mathcal{M}_P^T} = [(\boldsymbol{b_P} - \boldsymbol{a_P})^{\intercal}, (\boldsymbol{c_P} - \boldsymbol{a_P})^{\intercal}, (\boldsymbol{d_P} - \boldsymbol{a_P})^{\intercal}, \boldsymbol{a_P}^{\intercal}] \quad (1)$$

These matrices allow us to directly map any physical point $\boldsymbol{p_P}$ inside $\boldsymbol{T_P}$ to its analogous tetrahedron $\boldsymbol{T_V}$, by computing its local coordinates in $\boldsymbol{T_P}$ and mapping the point to the same coordinates in the equivalent tetrahedron $\boldsymbol{T_V}$:

$$\boldsymbol{p_V} = \boldsymbol{\mathcal{M}_V^T} \cdot (\boldsymbol{\mathcal{M}_P^T})^{-1} \cdot \boldsymbol{p_P} \quad (2)$$

By using this mapping strategy, the pair $\{\boldsymbol{T_P}, \boldsymbol{T_V}\}$ now identifies two equivalent volumes in **P** and **V**, even if their shape is different (as in Figure 3). Thus, not only physical vertices $\{\boldsymbol{a_P}, \boldsymbol{b_P}, \boldsymbol{c_P}, \boldsymbol{d_P}\}$ are mapped to their equivalent retargeted vertices $\{\boldsymbol{a_V}, \boldsymbol{b_V}, \boldsymbol{c_V}, \boldsymbol{d_V}\}$. Any other point inside $\boldsymbol{T_P}$ can also be mapped to its equivalent in $\boldsymbol{T_V}$ (e.g. a point on the edge $\overline{\boldsymbol{bc_P}}$ is mapped to point on the edge $\overline{\boldsymbol{bc_V}}$).

Bounding the interactive space: Physical and Visual trees

To build our space partitioning trees (we refer to them as tree **P** and tree **V**), we start by identifying the boundary of the interactive space around the user's torso in both spaces. We specifically approximate these as reduced icosahedrons, (with only 15 of the 20 tetrahedrons, as in Figure 4A and 4B). This geometry provides a basic structure, covering the space the user can reach with reduced complexity.

Let $\boldsymbol{T_P^i} = \{\boldsymbol{t_P}, \boldsymbol{p_{0P}}, \boldsymbol{p_{1P}}, \boldsymbol{p_{2P}}\} \subseteq \boldsymbol{P}$ and $\boldsymbol{T_V^i} = \{\boldsymbol{t_V}, \boldsymbol{p_{0V}}, \boldsymbol{p_{1V}}, \boldsymbol{p_{2V}}\} \subseteq \boldsymbol{V}$, with $\boldsymbol{i} \in [1,15] \subseteq \mathbb{N}$, describe each of the 15 equivalent tetrahedrons in both spaces. Point $\boldsymbol{t}$ identifies the user's torso and the mapping between boundary points is computed as $\boldsymbol{p_{jV}} = \boldsymbol{\mathcal{M}_V^P} \cdot \boldsymbol{p_{jP}}$, $j \in \{0,1,2\}$ (i.e. usual VR mapping described earlier). We use these 15 tetrahedrons to produce the two basic tree structures for **P** and **V**, with each tree containing 15 nodes in their first level and each tetrahedron node $\boldsymbol{T_P^i}$ in tree **P** having an analogous tetrahedron node $\boldsymbol{T_V^i}$ in tree **V** (shown in Figure 1C).

This tree structure is the seed for our multi-object retargeting mapping. Any point $\boldsymbol{p_P}$ around the user will be inside a unique leaf tetrahedron node $\boldsymbol{T_P^i}$ in tree **P**. Thus point $\boldsymbol{p_P}$ can be mapped to space **V** using $\boldsymbol{T_V^i}$, as in Eq(2).

As each boundary vertex in tree **P** has simply been multiplied by $\boldsymbol{\mathcal{M}_V^P}$ to compute its matching vertex in **V**, the

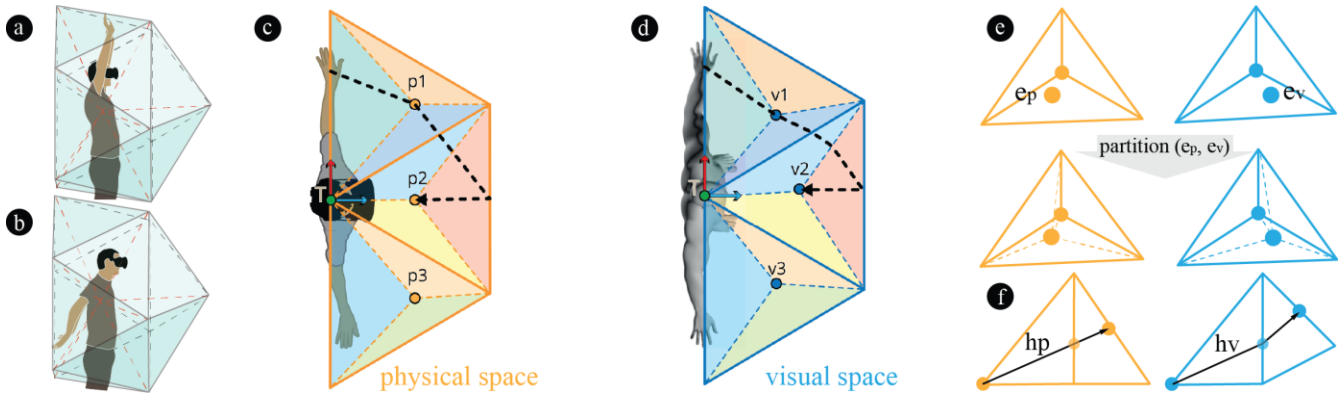

Figure 4. Summary of our manipulation technique. (A&B) Side 3D view of the boundary space enclosing user's interactive range. (C&D) Tetrahedron-based partitioning of the physical and visual space (simplified 2D view). Matching tetrahedrons highlighted on same colours. (E) An interactive element inside a tetrahedron will cause it to be sub-divided in four tetrahedrons. (F) Continuity of interaction is assured when hand moves across tetrahedrons, but the direction and speed of motion can be affected.

tetrahedron pairs have the same shape and our technique behaves like a traditional virtual hand (i.e. this is how the technique works if no interactive elements are within user's reach). Thus, current trees **P** and **V** act simply as an encapsulating boundary, allowing users to reach any point in **P** and **V**, but not the points beyond their natural reach.

The following subsection will modify this initial behaviour, by adding the interactive (retargeted) elements to the basic tree structure. Each interactive element will add internal tetrahedron pairs, but their shapes will not match (see example in Figure 4C and 4D). Thus, the volume inside the basic encapsulating boundary will be distorted, to accommodate the retargeted interactive elements.

Retargeted Space Partitioning

We iteratively partition the basic tree described above (15 tetrahedrons pairs, vertices on the boundary), adding each of the interactive elements within user's reach. Let Ɛ be the set of interactive elements. We model each element as a pair $\boldsymbol{e} = \{\boldsymbol{e_P}, \boldsymbol{e_V}\} \in Ɛ$, describing its coordinates in the visual and physical/retargeted spaces (the way we compute the pairs in set Ɛ is explained in the next section).

For each point $\boldsymbol{e_P}$, we determine the leaf tetrahedron node $\boldsymbol{T_P}$ it belongs to, subdivide it into four sub-tetrahedrons (as shown in Figure 4E), and add the corresponding nodes to tree structure **P**. Each new sub-tetrahedron uses $\boldsymbol{e_P}$ as its first vertex (origin of coordinates, fourth column in Eq(1)), and 3 of the 4 vertices in $\boldsymbol{T_P}$**.** The former leaf node $\boldsymbol{T_P}$ will keep a reference to $\boldsymbol{e}$ (and we will say *"*$\boldsymbol{T_P}$ *manages* $\boldsymbol{e}$").

Next, for each sub-tetrahedron added to tree **P**, we create its paired sub-tetrahedron $\boldsymbol{T_V}$ in tree **V**. Thus we use $\boldsymbol{e_V}$ as the first point and equivalent vertices in $\boldsymbol{T_V}$ (see Figure 4E), to ensure each sub-tetrahedron in tree **P** remains equivalent to its paired sub-tetrahedron in tree **V**.

This process produces the final equivalent tree structures for **P** and **V** (shown in Figure 4C&D). Tree **P** maintains a hierarchical space partitioning structure. If a point is inside a tetrahedron node, it is also inside its parent's tetrahedron, but not inside any of the parent's siblings. This allows for efficient mapping of users' physical hand locations to retargeted visual locations, by finding the leaf node in tree **P** the hand is inside and mapping it to space **V** as in Eq. (2).

Also, neighbour tetrahedron nodes always share a common face (see Figure 4E). This ensures continuity in the mapping when the physical hand leaves a node in tree **P** and enters a neighbour. However, as the geometry of the equivalent tetrahedrons in **P** and **V** might differ, hand motion direction and speed can change (see Figure 4F). The effects redirections may have in an example hand trajectory are shown in Figure 4C and 4D (black path; redirections occur as the hand moves across tetrahedrons). However, our use of a minimum hierarchical topology of tetrahedrons (15 plus 4 per interactive element) minimizes the occurrence of these artefacts, and the fact that the hand is moving will reduce the chances of user's perceiving this change [14].

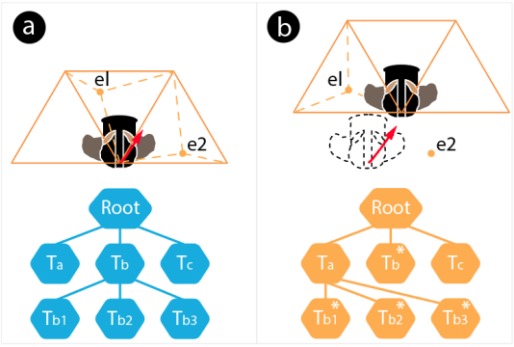

Figure 5: User displacements will change the mapping of interactive elements, causing the hierarchical tree structure to be recomputed.

Real time update of the trees.

The position of the interactive elements relative to the user will vary as this travels through the VE. This will require changes to the tree structure, to maintain the hierarchical space partitioning properties of tree **P** (see Figure 5).

In each frame, we start by marking all tree nodes as dirty, and define an (initially) empty set Ɛ'. We then proceed to iterate through the current set of interactive elements in Ɛ. For a given $\boldsymbol{e_P}$, managed by node $\boldsymbol{T_P}$, if $\boldsymbol{e_P}$ is still inside $\boldsymbol{T_P}$, this node and all of its children leaf nodes (i.e. not managing any other interactive element) are marked as clean. On the other hand, if $\boldsymbol{e_P}$ is inside a node other than $\boldsymbol{T_P}$, we add *e* to Ɛ' and remove it from Ɛ.

At the end of this process all dirty nodes' children are removed from the trees (see *e2* in Figure 5). Set Ɛ contains the elements which are still correctly located and are directly committed (i.e. update the location of tetrahedron's vertices). Finally, elements in Ɛ' are re-introduced, using the iterative approach described in the previous sub-section.

COMPUTING RETARGETING MAPPINGS

The approach above describes a manipulation technique that can provide retargeted manipulation for a set of multiple interactive elements (given their physical and corresponding visual locations). The challenge still remains to find the optimum mapping Ɛ for these points, based on ergonomics, spatial criteria and mismatch thresholds of visual dominance. Please note that only interactive elements (set Ɛ) are retargeted. Boundary points remain unaffected, to maintain the size of the user's reachable space.

As a first step to guide our retargeting approaches, we need to describe the metrics that will assess the quality of a retargeting mapping Ɛ. We then report two example approaches to compute the retargeting mapping based on these metrics and different criteria.

Quantifying retargeted mappings

Our algorithms will make use of three factors to evaluate the quality of the potential retargeting mappings. The final cost function for a mapping is computed as a weighted average, with the specific value of the weights depending on the retargeting approach used:

$$C(\mathcal{E}) = w_1 \cdot R\_S(\mathcal{E}) + w_2 \cdot V\_S(\mathcal{E}) + w_3 \cdot S\_S(\mathcal{E}) \quad (3)$$

Adapted continuous RULA (R_S()):
We use a metric inspired in the four first steps of the RULA process, as these are the steps providing an ergonomic score based on the position of the arms, which is the space our manipulation technique addresses.

Being initially an observational method, RULA uses broad ranges for the orientation of each joint, providing a discrete score for each range (e.g. a shoulder between ±20º, is ranked as +1; 20-45º, is ranked as +2, etc.), with a final score for each arm between 1-9, associated to a risk level (neglectable, low, medium or high risks; associated areas for these scores are visible in Figure 2.A and C).

This scheme allowed assessment of workers performing manual tasks through pictures or videos. However, when combined with our optimization methods, this results in a staircase function, with searches getting stuck in plateaus until the next step is reached (a change in RULA score). This then resulted in sudden changes in the retargeting mapping (e.g. when a user approached an interactive element, big changes in retargeting happened as it transitioned from one RULA score to the next one).

To prevent this and allow for smooth retargeting schemes, we simply take each angular range for each of the joints, and apply linear interpolation between the joint angle and the RULA scores for that range and joint. Then, for any given a point e_P, we used an IK algorithm (IKAN [44]) to compute the angles of the three arm joints, keeping the angles providing most ergonomic (lower) score for disambiguation. The global score for a given mapping $\mathcal{E}$ is then simply computed as $R\_S(\mathcal{E}) = \sum_{\{e_P, e_V\} \in \mathcal{E}} R\_S(e_P)$.

Please note this modified RULA score is used to compute mappings only. Our study used the usual RULA scores.

Visual dominance mismatch threshold (V_S(ℰ)):
In our study we explore the use of ERG-O for VR retargeted interaction, without making use of any type of tactile feedback. As such, the thresholds reported by Burns et al. [14] (up to 20cm) could be used. We however took a more conservative maximum mismatch of 10 cm, penalizing retargeting pairs where the distance between the visual and physical elements were likely to be detected. Thus, we defined our metric as $V\_S(\mathcal{E})) = \sum \|e_P - e_V\|$, $\forall \{e_P, e_V\} \in \mathcal{E} \,/ \|e_P - e_V\| > 10cm$.

Spatial relationship preservation (S_S(ℰ)):
Our manipulation technique can map **V** and **P** spaces, based on any set of point pairs. This could result in mappings in **P** space that hold not relation to the way elements are arranged in **V** space. This metric penalizes mappings where the ratio of distances between physical pairs and visual pairs is not constant, as a way to preserve the topology between elements.

To do so, for each two points $a,b \in \mathcal{E}$, we measure their distance in **P** and distance in **V** and compute their ratio $r(a,b) = \|a_P - b_P\| / \|a_V - b_V\|$. To model that this ratio should be similar among all pairs (and penalize otherwise), we define *S_S(ℰ)* as *"the variance in* $r(a,b), \forall a,b \in \mathcal{E}$*"*.

Optimization methods to compute mappings
To illustrate our approach, we report two simple example approaches to compute retargeting mappings using the metrics described. The first approach is aimed at preserving the spatial structure between elements; while the second one loosens this criteria to reinforce ergonomics.

Spatial Consistent retargeting (S_R):
This first approach is designed to improve ergonomics and maintain mismatch threshold, but keeping the spatial relationships among the interactive elements intact (see second column in Figure 6) . To do so, we use a scale transformation matrix $\boldsymbol{S_P^V}$, centred on the user chest, to equally affect all interactive elements, with visual positions mapped to physical positions as $\boldsymbol{p_P} = \boldsymbol{S_P^V} \cdot \boldsymbol{p_V}$.

This problem is modelled using a single variable *k*, to represent the scaling factor applied by $\boldsymbol{S_P^V}$. Let $\boldsymbol{t_V}$ be the position of the user's torso and $\{\boldsymbol{e_P}, \boldsymbol{e_V}\} \in \mathcal{E}$ the most distant element to $\boldsymbol{t_V}$. If $k \in (0, \|e_V - t_V\|)$, all elements will stay within the reachable volume.

This technique uses a naïve linear search, testing 2000 potential *k* values within this interval to find the value that minimizes the cost function shown in Eq(3). Weights were empirically tuned to $w_1 = 0.3$, $w_2 = 0.7$, with the last factor being ignored ($w_3 = 0$), as this retargeting strategy inherently maintains spatial relationships.

This technique should not be mistaken for a simple motor-space scaling method. Only the interactive elements are retargeted, and the boundary still encloses all the reachable space. Thus, redirections (Figure 3F) will still affect the hand (e.g. in our study, every time the user reaches from the belly to the target, or when reaching targets from the side).

Ergonomic Retargeting (E_R):
This approach optimizes the position of each $\{e_P, e_V\} \in \mathcal{E}$ independently. This loosens the constraints on spatial preservation from the previous approach, in order to achieve higher improvements for ergonomics.

This problem is modelled as a multivariable optimization approach, one for each of the XYZ coordinates of the $\boldsymbol{e_P}$ elements in $\mathcal{E}$. We make use of Simulated Annealing (SA), a probabilistic technique for approximating the global optimum of our cost function [8, 16]. The weights of the cost functions were empirically tuned to $w_1 = 0.2$, $w_2 = 0.4$ and $w_3 = 0.4$. Neighbours are computed by jittering a physical point $\boldsymbol{e_P}$ in the current mapping $\mathcal{E}$ with a random direction and magnitude, for a maximum displacement of 5 cm (50% of our mismatch threshold). Transition acceptance between mappings follows the method by Kirkpatrick [25]. Let $\mathcal{E}_1$ and $\mathcal{E}_2$ be two potential mappings, *C(ℰ)* be our cost function and *T* the current temperature. The probability of transitioning to from $\mathcal{E}_1$ to $\mathcal{E}_2$.is computed as in Eq(4).

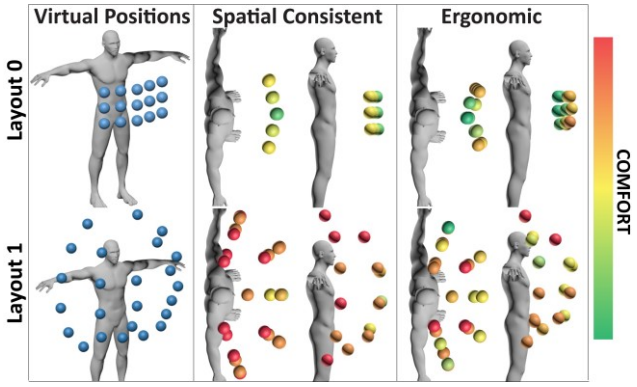

Figure 6: Comparison of the retargeting behaviour of each of our approaches, for two different layouts.

$$P(\mathcal{E}_1, \mathcal{E}_2, T) = \begin{cases} 1 & , C(\mathcal{E}_2) < C(\mathcal{E}_1) \\ e^{\frac{C(\mathcal{E}_1) - C(\mathcal{E}_2)}{T}} & , C(\mathcal{E}_2) \geq C(\mathcal{E}_1) \end{cases} \quad (4)$$

Our cooling schedule uses *Ns*=10 step adjustments per temperature step, *Nt* =5 temperatures steps per temperature change, cooling factor *Rt* =0.5 and initial temperature *T*=180, testing nearly 18.000 possible retargeting mappings per optimization (frame). The results (best mapping) from a frame are used as the starting state for the next frame, as user displacements are likely to be small from frame to frame. This allowed us to produce satisfying results, while maintaining the real-time requirements of ERG-O, even with the relatively aggressive cooling schedule used.

Analytical comparison of retargeting approaches

In this section we analyse the differences in retargeting introduced by each of our example strategies. Figure 6 shows two examples of interactive elements around the user. In the first example (top), the visual elements (in blue) are already at comfortable locations within user reach. In the second example, the interactive elements are evenly located around the user, close to the limits of its reachable space. Generally these are uncomfortable positions, especially for lowest points and points above user's chest.

As expected, *Spatial Consistent* retargeting (*S_R*) repositions elements maintaining their spatial structure, while *Ergonomic Retargeting* (*E_R*) affects structure, in order to enable more ergonomic interaction.

For the first example, *S_R* performed minor corrections (the displacement between visual and retargeted points within AVG + 6.8cm, STDEV 6.1cm), but still achieved improvements in ergonomics. The behaviour of *E_R* is more interesting. Although the retargeted distances were similar (AVG + 8.3cm, STDEV 8.6cm), the figure (top, right) shows how *E_R* flipped the structure of the elements (i.e. from a concave to a convex shape). The resulting shape actually wraps around the central part of the ergonomic area (note the shape of RULA zones in Figure2.C), achieving much higher improvements.

This behaviour can be explained by looking at our definition of *S_S(Ɛ)*. By flipping the shape, the ratio of the distances between any two pair of points is actually preserved. This allowed (*E_R*) to significantly improve ergonomic score for the nine central elements, although at the expense of decreasing the score of the elements at the edges. The wrapping to a curved shape shows *E_R*'s efforts to bring this edges back to more ergonomic locations, but metric *S_S(Ɛ)* did penalize this wrapping.

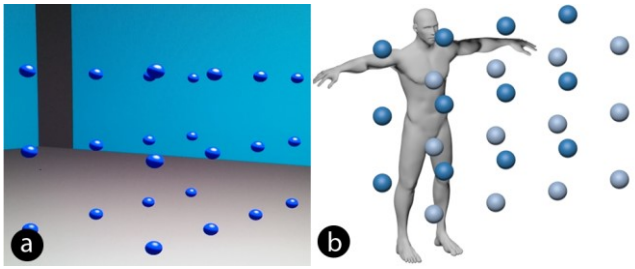

Figure 7: (A) Screenshot showing the selection task implemented in out testing environment and (B) third layout tested, with visual elements anchored to the world in two planes, and forcing users to walk in order to reach them.

For the second example (second row in Figure 6) *S_R* shows a similar behaviour as in the first example (6.9 ± 6.5cm), while *E_R* presents a more aggressive behaviour (10.1±9.5cm), specially the positions of low and high points (least comfortable). As expected, this results in higher ergonomic gains for *E_C*, but also higher spatial distortion.

USER STUDY

The previous sections motivate the need for Erg-O and provide a formal definition for the technique. The current section will evaluate the usability of the technique in a VR selection task. We compare our two examples of retargeting strategies against a traditional virtual hand technique, to gain insight on the improvements obtained for ergonomic interaction and the influence that distortions (due to retargeting and space warping) could have on interaction.

Task and Environment

We implemented a target selection task to test our technique, with 30 trials per task. At the beginning of each trial, users could see a range of blue spheres (i.e. interactive elements) floating in the space in front of them. Two spheres were highlighted in green (instead of blue), to inform users of the targets of their selection, and a regressive countdown from 5 to 0 was shown. When the countdown finished, users touched their belly to select the hand they wanted to use for that trial, and proceeded to touch the highlighted spheres. An auditive cue notified users when they had correctly selected each target. The pair of spheres to select was randomly chosen, but both spheres were reachable with a single hand.

The environment was implemented using C++ and OpenGL. We used an Oculus Rift DK2 for display, OptiTrack to achieve a larger tracking volume and Kinect v2 for skeletal tracking. Projection matrices and barrel distortion meshes were replicated from Oculus SDK v1.7. Conventional speakers were used for audio feedback.

Layouts tested:

We tested the techniques using three different layouts, to assess their performance under several usage scenarios. In some layouts (L1 and L2) we wanted spheres to stay in specific areas relative to the user (e.g. in comfortable/ uncomfortable points). In these cases, the grid of spheres was anchored to the users' lower torso, so that they would stay at these fixed areas even if the users moved. Upper torso (i.e. chest) was avoided as an anchor, as its orientation can change when users reach towards an object due to accompanying movement of the shoulder.

During tests, we measured users' arm span A. All distances and positions describing our layouts are relative to A, but in our explanations we will report the equivalent value in centimetres for a reference user with A=170 cm.

Ergonomic Layout (L1)

This layout (shown earlier in Figure 6) consisted of 15 spheres, placed in a 5x3 grid in front of the user's lower torso and at a distance of 0.21·A (~36 cm). This is an agreed zone for comfortable interaction (e.g. middle ground between the comfortable plane used in [23] and the volume receiving a RULA score of 1). This was chosen as a worst case scenario to test against our technique, because: a) there is little room for improvement due to ergonomic retargeting (spheres are already at comfortable locations); and b) users will still suffer from the distortions and loss of linearity (Figure 4F) introduced by our retargeting strategies.

Limits of Reach Layout (L2)

This second layout (also displayed in Figure 6) consisted of 24 spheres, evenly distributed along the limits of users' reachable space at 0.44A (~75 cm) and anchored to the users' lower torso, as above. In contrast to L1, this layout should provide best ergonomic improvements, but at the same time, it will introduce more aggressive retargetings. This can increase spatial distortion, which could hinder motor control and affect the selection task. Thus, L2 should help illustrate the extent of the benefits of Erg-O for ergonomics and the impact of its redirections.

World Fixed Layout (L3)

This last layout (shown in Figure 7B) is based on a more generic scenario were elements are fixed in the VE (instead of anchored to the user) and distributed across a bigger volume, forcing users to walk to them in order to interact with them. More specifically, 24 spheres were evenly distributed over two vertical planes, spanning across 1.4Ax0.8A (238 cm x 136 cm). Lowest and highest spheres were placed at heights 0.4A (68 cm) and 1.2A (204 cm) from the floor, forcing users to reach both low points and points above their heads. Both planes were separated by a distance of 0.5A (85 cm), ensuring element in one plane would not be in reach from the other plane. Besides testing a more generic scenario, this layout allowed us to see the influence of a varying retargeted mapping (i.e. the retargeting for each sphere changed as user moved, as this changed the sphere's position relative to the user).

Experimental Design

In the experiment, we compared three techniques: Natura virtual hand (*N*), Spatial Consistent retargeting (*S_R*) and Ergonomic retargeting (*E_R*). We adopted a 3x3 full factorial design, with factors being the technique (*N*, *S_R* or *E_R*) and layout (*L1*, *L2* or *L3*), counterbalanced following a Latin Square design.

The experiment was conducted with 12 participants (10 male, and 2 female between the ages of 21 and 35. We collected 3240 trials (12 participants, 9 blocks, 30 trials each). Each participant was tested individually and the experiment took approximately 45 minutes per participant.

Dependent Variables measured

Participants were asked to fill a user comfort and physical effort questionnaires after each block (technique).

The experimental software recorded: trial completion time (TCT), and the length of the real (RP) and virtual hand paths (RP) for each trial. TCT measured the time between the user touching the first and second highlighted spheres. Path lengths (RP and VP) were measured as the ratio between the length of the path followed by the (real or virtual) hand, divided by the linear distance between the spheres [48]. This allowed comparisons across paths of different lengths and measured effectiveness (deviation from optimum) for the interaction. Conventional RULA scores were also recorded when users selected each sphere, to test if our mappings actually improved ergonomics.

RESULTS AND ANALYSIS

For all analysis presented in this section a repeated measures ANOVA was conducted to compare the effect of the 3 techniques (Natural (*N*), Spatial Consistent (*S_R*) and Ergonomic (*E_R*)) on mean time, effort and path length. Outliers were filtered out (i.e. mean ± 2 standard deviation), removing 284 trials (2.83% of samples). Post-hoc comparisons used Bonferroni corrections for each case.

We start the analysis by looking at the general behaviour of each retargeting approach, and then focus our analysis on each of the different layouts tested, to get further insight on how the approaches behave in different scenarios.

General analysis of retargetting approaches

Retargeting Approach vs Time

Results showed a significant effect on the average time required to complete the selection task ($F(2,4)=279.67$, $p<0.001$), depending of the type of retargeting. Post-hoc comparisons using Bonferroni corrections showed significant differences. Specifically *S_R* (M=0.945s, SD=0.473s) was faster TCT than *E_R* (M= 1.043, SD= 0.473s), p= 0.001; and also faster than *Natural* (M= 1.03s, SD= 0.734s), p= 0.005. No such differences were found between *E_R* and *Natural*, p= 1. These findings suggest that *E_R* and *Natural* conditions behave in a very similar way, but the use of the *Spatial Consistent* retargeting approach can lead to lower task execution times.

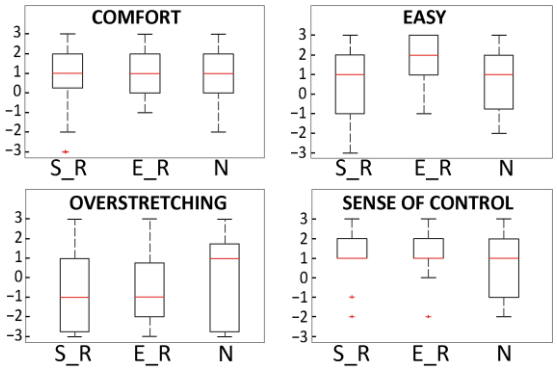

Figure 8: Box plots for the results of our questionnaires. Horizontal red bars represent medians, and boxes represent the interquartile ranges (IQRs). Whiskers stretch to the data points that are within the median ± 1.5 IQR.

Retargeting Approach vs Comfort

Results showed a significant effect on comfort $F(2,4)=26.06$, $p<0.001$ depending of the retargeting approach used. Post-hoc tests with Bonferroni corrections show significant difference ($p=0.002$) between *E_R* ($M=1.6078$, $SD=1.0934$) and *Natural* ($M=1.7767$, $SD=1.1175$). No other differences in comfort were found. This result suggests that using the *Ergonomic (E_R)* retargeting approach can reduce user effort, possibly enabling longer usage periods before the user gets tired.

Retargeting Approach vs Length

This analysis showed no effects of retargeting type on path length performance. This could indicate that the thresholds used to optimize the target positions (~10cm) were too small compared to the hand displacements required to complete the task, as to represent a significant difference.

Retargeting Approach vs Self Reports

Figure 8, shows the results of the questionnaires filled after each retargeting condition block (*S_R*, *E_R* and *Natural*). We used a Likert scale from -3 to 3 to assess the comfort, easiness of reachability, sense of control and overstretching. The boxes represent the interquartile ranges (IQRs) and the whiskers represent the confidence interval.

Participants perceived all techniques as similar in terms of comfort, which indicates that the blocks were not long enough as to make the improvements to ergonomics (RULA) become a driving factor for effort in this task.

Approach *E_R* was perceived as the approach allowing easier reachability and less overstretching. More interesting, users reported that they felt more control when using any of the retargeted conditions (*S_R* or *E_R*) than using *N*.

This could be a result of both *S_R* and *E_R* placing the objects at slightly closer physical positions of each other. This would cause the index of difficulty of the task (Fitt's law) to decrease, making them easier to reach and potentially affecting the users' assessment about their sense of control. However, as no significant differences were found for path length (hand motion not significantly shorter than in *N*), we cannot strongly support this hypothesis.

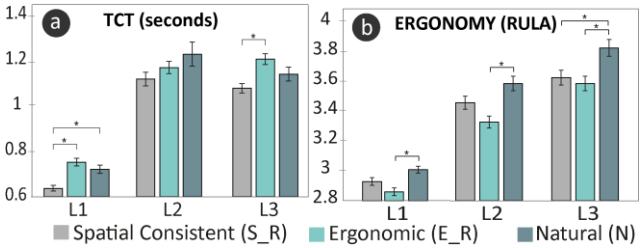

Figure 9: Average measurements per strategy and layout: (a) Time completion task and (b) RULA scores during the task. Significant difference between retargeting strategies for each layout are represented by '*'.

In any case, the fact that *S_R* or *E_R* did not actually receive worse scores for control was found a very positive result. This seems to indicate that the spatial distortion and the artefacts related to linearity (Fig 3F) still allow fluent interaction, confirming our empirical observations.

Retargeting approach vs Layout

Layout 1

The results showed a significant effect of retargeting on TCT ($F(2,4)=12.295$, $p<0.001$), for Layout 1. Post-hoc comparisons showed significant differences in time, with *S_R* ($M=0.640$s, $SD=0.234$s) leading to lower TCT than either *E_R* ($M= 0.749$s, $SD= 0.316$s), $p< 0.001$; or *Natural* conditions ($M= 0.722$s, $SD= 0.348$s), $p= 0.001$.

Retargeting approach also influenced Comfort ($F(2,4)= 8.92$, $p<0.001$). Pairwise comparisons showed significant differences, with *E_R* ($M= 2.86$, $SD= 0.502$) providing better scores than *N* ($M=3.01$, $SD=0.529$), $p<0.001$, even if objects in Layout 1 were already at comfortable positions.

These results confirm general expectations about *S_R* and *E_R*, with the first one improving performance, while the second one improved comfort. However, *E_R* not being faster than *N* could indicate *E_R* was not good for performance. The objects being at more comfortable locations, and the arguably smaller index of difficulty of the task, should both benefit *E_C* for *TCT*. We believe the more aggressive redirections could make users rely more on visual feedback, making them perform more slowly.

Layout 2

Our results showed no significant effect of approach on TCT ($F(2,4)=2.664$, $p=0.07$) for Layout 2. Retargetting a few centimeters was probably not a significant advantage for the longer hand displacements required in this task.

The analysis however showed significant effects on Comfort ($F(2,4) = 8.238$, $p<0.001$), with paired analysis indicating that *E_R* ($M=3.33$, $SD=0.75$) led to better comfort than *Natural* ($M=3.59$, $SD=0.932$), $p<0.001$, and confirming the general trend of these techniques, also for scenarios involving large arm movements.

Layout 3

Retargeting strategy showed significant effects for both TCT ($F(2,4)=5.628$, $p=0.004$) and Comfort ($F(2,1077)= 5.902$, $p=0.003$) in this layout. Post-hoc comparisons

showed participants were faster using *S_R* (M=1.08s, SD= 0.385s) than with *E_R* (M= 1.2s, SD= 0.437s), p= 0.002, but no significance was found compared to *N* (p= 0.282).

In terms of comfort, the scores were generally high (uncomfortable). *Natural* (M=3.83, SD=1.076) led to worse results than either *E_R* (M=3.59, SD=0.924), p=0.005, or *S_R* (M=3.63, SD=0.950), p=0.02. We observed users tended to walk towards the targets with their arms fully extended (i.e. focusing on performance, rather than interacting comfortably), which probably blurred the differences between techniques. However, instructing participants to interact comfortably (rather than quickly) could have produced a similar bias (i.e. walk until the target is in comfortable reach and then select; this would also result in no differences in comfort across techniques). Instructing them to walk to specific points before selecting, would have implicitly fixed the location of targets relative to the user, blurring differences with L1 and L2.

DISSCUSION

The approach described (Erg-O) uses controlled warping of the visual and physical space around the user, to enable multi-object retargeting in an open-ended fashion. Our two example retargeting functions (*E_R* and *S_R*) also helped us illustrate how Erg-O can be used to improve ergonomic interaction in VR. Is spite of warping space (i.e. virtual hand not following the exact motion of the real hand), both strategies improved ergonomic scores without decreasing performance (actually, *S_R* resulted in better TCT than N for some scenarios); sense of control or complexity.

Our example strategies also highlight the importance of the retargeting function. First, they can result in very different behaviours (*S_R* being generally better for TCT, while *E_R* improved ergonomics). Using other metrics for ergonomic assessment (e.g. Jack [3] or [23]), other functions or weight distributions could produce different results. Second, even simple functions, such as *S_R*, can produce good results.

The importance of spatial preservation was also highlighted (see artefacts produced by *E_R*, in Figure 6). For example, consider two elements, with A visually to the left of B. A function retargeting B to the left of A would result in undesirable discontinuities for interaction. Similarly, tetrahedron pairs with very different shapes or volumes would result in strong redirections and significant changes in speed, and the retargeting function should avoid this.

Beyond the examples presented in this paper (multi-object retargeting to improve ergonomics in VR), varying specific aspects of Erg-O can adapt it to other application scenarios.

For instance, boundaries **P** and **V** were kept equal and always anchored to the user's and avatar's chest. Scaling the boundary in **V**, would enable interaction with distant objects in the VE (i.e. similar to Go-Go, but allowing multi-object retargeting inside). Detaching tree **V** from the user's chest and moving it to a distant point of the VE could replicate the HOMER [11] technique.

Also, unlike in the example presented in the paper, the shape of the boundaries **P** and **V** do not need to match. This could be useful for users with limited limb mobility, as the boundaries of tree **P** can be tailored to circumscribe the physical space the patient can reach. Tree **V** could still circumscribe the reachable space for a person with normal mobility, and our isomorphic mapping would allow patients with reduced mobility to interact within all this space.

The internal topology of the tree (retargeted points and resulting tetrahedrons) could be used to further refine this mapping. In the case of users with limited mobility this could be used to avoid uncomfortable poses or to provide adequate levels of resolution to specific parts of the space, based on the patient's motor skills and condition. As a particular example, this could apply to children with mental palsy or spasticity, to create novel range of motion exercises [20] or building games (e.g. LEGO) exploiting the spatial properties of VR to improve cognitive skills [18].

Taking the opposite approach, the retargeting strategy could be tailored to force specific poses in the patient (e.g. most of the visual space mapped to higher locations in the user's physical space, forcing the user to lift his arms). This could be applied for rehabilitation or physical training purposes.

Our solution could also be applied to surgical simulations, such as [42], in which retargeting is currently limited to two dimensional surfaces.

CONCLUSION

In this paper, we presented Erg-O, a multi-object retargeting technique for manipulation in VR. The visual location of one or more interactive objects (e.g. buttons) is maintained, but users can reach them from more ergonomic locations. Users can move their hands freely, and they can also reach any other points (not only retargeted elements). We achieve this by creating a mapping between he visual and physical space that warps the user's reachable space according to the location of the retargeted elements.

We presented a formalization of our manipulation technique, and also described two example retargeting strategies to compute the best physical retargeted positions for interactive elements, according to spatial and ergonomic criteria. We finally evaluated the performance of these example retargeting techniques compared to a traditional virtual hand (baseline). Results from our study demonstrated the potential of our technique to improve ergonomics, without significant effects on performance or sense of control. We finished the paper by discussing relevant aspects related to the use of Erg-O in other scenarios, as well as identifying other possibilities and application scenarios where Erg-O can be applied.

ACKNOWLEDGEMENTS

This work has been supported by Mexican National Council of Science and Technology (CONACyT). We thank Luis Veloso for his help in creating the figures and editing the accompanying video figure.

REFERENCES

1. Azmandian, Mahdi, Mark Hancock, Hrvoje Benko, Eyal Ofek, and Andrew D Wilson. *Haptic retargeting: Dynamic repurposing of passive haptics for enhanced virtual reality experiences*. in *Proceedings of the 2016 CHI Conference on Human Factors in Computing Systems*. 2016. ACM. DOI: http://dx.doi.org/10.1145/2858036.2858226
2. Bachynskyi, Myroslav, Gregorio Palmas, Antti Oulasvirta, and Tino Weinkauf, *Informing the design of novel input methods with muscle coactivation clustering.* ACM Transactions on Computer-Human Interaction (TOCHI), 2015. **21**(6): p. 30. DOI: http://dx.doi.org/10.1145/2687921
3. Badler, Norman I, Cary B Phillips, and Bonnie Lynn Webber, *Simulating humans: computer graphics animation and control*. 1993: Oxford University Press,
4. Ban, Yuki, Takashi Kajinami, Takuji Narumi, Tomohiro Tanikawa, and Michitaka Hirose. *Modifying an identified curved surface shape using pseudo-haptic effect*. in *Haptics Symposium (HAPTICS), 2012 IEEE*. 2012. IEEE. DOI: http://dx.doi.org/10.1007/978-3-642-31401-8_3
5. Banakou, Domna, Raphaela Groten, and Mel Slater, *Illusory ownership of a virtual child body causes overestimation of object sizes and implicit attitude changes.* Proceedings of the National Academy of Sciences, 2013. **110**(31): p. 12846-12851. DOI: http://dx.doi.org/10.1073/pnas.1306779110
6. Banakou, Domna and Mel Slater, *Body ownership causes illusory self-attribution of speaking and influences subsequent real speaking.* Proceedings of the National Academy of Sciences, 2014. **111**(49): p. 17678-17683. DOI: http://dx.doi.org/10.1073/pnas.1414936111
7. Barbagli, Federico, Ken Salisbury, Cristy Ho, Charles Spence, and Hong Z Tan, *Haptic discrimination of force direction and the influence of visual information.* ACM Transactions on Applied Perception (TAP), 2006. **3**(2): p. 125-135. DOI: http://dx.doi.org/10.1145/1141897.1141901
8. Bertsimas, Dimitris and John Tsitsiklis, *Simulated annealing.* Statistical science, 1993. **8**(1): p. 10-15. DOI: http://dx.doi.org/10.1214/ss/1177011077
9. Borg, Gunnar, *Borg's perceived exertion and pain scales*. 1998: Human kinetics,
10. Boring, Sebastian, Marko Jurmu, and Andreas Butz. *Scroll, tilt or move it: using mobile phones to continuously control pointers on large public displays*. in *Proceedings of the 21st Annual Conference of the Australian Computer-Human Interaction Special Interest Group: Design: Open 24/7*. 2009. ACM. DOI: http://dx.doi.org/10.1145/1738826.1738853
11. Bowman, Doug A and Larry F Hodges. *An evaluation of techniques for grabbing and manipulating remote objects in immersive virtual environments*. in *Proceedings of the 1997 symposium on Interactive 3D graphics*. 1997. ACM. DOI: http://dx.doi.org/10.1145/253284.253301
12. Bricken, Meredith, *Virtual reality learning environments: potentials and challenges.* ACM SIGGRAPH Computer Graphics, 1991. **25**(3): p. 178-184. DOI: http://dx.doi.org/10.1145/126640.126657
13. Burdorf, Alex and Judith Laan, *Comparison of methods for the assessment of postural load on the back.* Scandinavian journal of work, environment & health, 1991: p. 425-429, URL: http://www.jstor.org/stable/40965930
14. Burns, Eric, Sharif Razzaque, Abigail T Panter, Mary C Whitton, Matthew R McCallus, and Frederick P Brooks. *The hand is slower than the eye: A quantitative exploration of visual dominance over proprioception*. in *Virtual Reality, 2005. Proceedings. VR 2005. IEEE*. 2005. IEEE. DOI: http://dx.doi.org/10.1109/VR.2005.1492747
15. Bustamante, Ernesto A and Randall D Spain. *Measurement invariance of the Nasa TLX*. in *Proceedings of the Human Factors and Ergonomics Society Annual Meeting*. 2008. SAGE Publications Sage CA: Los Angeles, CA. DOI: http://dx.doi.org/10.1177/154193120805201946
16. Černý, Vladimír, *Thermodynamical approach to the traveling salesman problem: An efficient simulation algorithm.* Journal of optimization theory and applications, 1985. **45**(1): p. 41-51. DOI: http://dx.doi.org/10.1007/BF00940812
17. Cheng, Lung-Pan, Eyal Ofek, Christian Holz, Hrvoje Benko, and Andrew D Wilson. *Sparse Haptic Proxy: Touch Feedback in Virtual Environments Using a General Passive Prop*. in *Proceedings of the 2017 CHI Conference on Human Factors in Computing Systems*. 2017. ACM.DOI: 10.1145/3025453.3025753
18. Cheng, Yi-Ling and Kelly S Mix, *Spatial training improves children's mathematics ability.* Journal of Cognition and Development, 2014. **15**(1): p. 2-11. DOI: http://dx.doi.org/10.1080/15248372.2012.725186
19. Colman, Andrew M, *A dictionary of psychology*. 2015: Oxford University Press, USA,
20. Dunne, Alan, Son Do-Lenh, Gearóid Ó'Laighin, Chia Shen, and Paolo Bonato. *Upper extremity rehabilitation of children with cerebral palsy using accelerometer feedback on a multitouch display*. in *Engineering in Medicine and Biology Society (EMBC), 2010 Annual*

International Conference of the IEEE. 2010. IEEE. DOI: http://dx.doi.org/10.1109/IEMBS.2010.5626724

21. Dünser, Andreas, Karin Steinbügl, Hannes Kaufmann, and Judith Glück. *Virtual and augmented reality as spatial ability training tools*. in *Proceedings of the 7th ACM SIGCHI New Zealand chapter's international conference on Computer-human interaction: design centered HCI*. 2006. ACM. DOI: http://dx.doi.org/10.1145/1152760.1152776
22. Flasar, Jan. *Interaction Techniques for Object Selection/Manipulation in Non-Immersive Virtual Environments with Force Feedback*. 2001. Eurohaptics, URL:http://www.eurohaptics.vision.ee.ethz.ch/2001/flasar.pdf
23. Hincapié-Ramos, Juan David, Xiang Guo, Paymahn Moghadasian, and Pourang Irani. *Consumed endurance: a metric to quantify arm fatigue of mid-air interactions*. in *Proceedings of the 32nd annual ACM conference on Human factors in computing systems*. 2014. ACM. DOI: http://dx.doi.org/10.1145/2556288.2557130
24. Kilteni, Konstantina, Jean-Marie Normand, Maria V Sanchez-Vives, and Mel Slater, *Extending body space in immersive virtual reality: a very long arm illusion.* PloS one, 2012. **7**(7): p. e40867. DOI: http://dx.doi.org/10.1371/journal.pone.0040867
25. Kirkpatrick, Scott, C Daniel Gelatt, and Mario P Vecchi, *Optimization by simulated annealing.* science, 1983. **220**(4598): p. 671-680, URL: http://www.jstor.org/stable/1690046
26. Kohli, Luv, Mary C Whitton, and Frederick P Brooks. *Redirected touching: The effect of warping space on task performance*. in *3D User Interfaces (3DUI), 2012 IEEE Symposium on*. 2012. IEEE. DOI: http://dx.doi.org/10.1109/3DUI.2012.6184193
27. Kohli, Luv. *Redirected touching: Warping space to remap passive haptics*. in *3D User Interfaces (3DUI), 2010 IEEE Symposium on*. 2010. IEEE. DOI: http://dx.doi.org/10.1109/3DUI.2010.5444703
28. Kokkinara, Elena, Konstantina Kilteni, Kristopher J Blom, and Mel Slater, *First Person Perspective of Seated Participants Over a Walking Virtual Body Leads to Illusory Agency Over the Walking.* Scientific Reports, 2016. **6**. DOI: http://dx.doi.org/10.1038/srep28879
29. Lee, Yongseok, Inyoung Jang, and Dongjun Lee. *Enlarging just noticeable differences of visual-proprioceptive conflict in VR using haptic feedback*. in *World Haptics Conference (WHC), 2015 IEEE*. 2015. IEEE. DOI: http://dx.doi.org/10.1109/WHC.2015.7177685
30. Lopez, Christopher, Pär Halje, and Olaf Blanke, *Body ownership and embodiment: vestibular and multisensory mechanisms.* Neurophysiologie Clinique/Clinical Neurophysiology, 2008. **38**(3): p. 149-161. DOI: http://dx.doi.org/10.1016/j.neucli.2007.12.006
31. Matsuoka, Yoky, Sonya J Allin, and Roberta L Klatzky, *The tolerance for visual feedback distortions in a virtual environment.* Physiology & behavior, 2002. **77**(4): p. 651-655. DOI: http://dx.doi.org/10.1016/S0031-9384(02)00914-9
32. McAtamney, Lynn and E Nigel Corlett, *RULA: a survey method for the investigation of work-related upper limb disorders.* Applied ergonomics, 1993. **24**(2): p. 91-99. DOI: http://dx.doi.org/10.1016/0003-6870(93)90080-S
33. Normand, Jean-Marie, Elias Giannopoulos, Bernhard Spanlang, and Mel Slater, *Multisensory stimulation can induce an illusion of larger belly size in immersive virtual reality.* PloS one, 2011. **6**(1): p. e16128. DOI: http://dx.doi.org/10.1371/journal.pone.0016128
34. Ott, Michela and Laura FREINA. *A literature review on immersive virtual reality in education: state of the art and perspectives*. in *Conference proceedings of» eLearning and Software for Education «(eLSE)*. 2015. Universitatea Nationala de Aparare Carol I, URL: https://www.ceeol.com/search/article-detail?id=289829
35. Plantard, Pierre, Edouard Auvinet, Anne-Sophie Le Pierres, and Franck Multon, *Pose estimation with a kinect for ergonomic studies: Evaluation of the accuracy using a virtual mannequin.* Sensors, 2015. **15**(1): p. 1785-1803. DOI: http://dx.doi.org/10.3390/s150101785
36. Poupyrev, Ivan, Mark Billinghurst, Suzanne Weghorst, and Tadao Ichikawa. *The go-go interaction technique: non-linear mapping for direct manipulation in VR*. in *Proceedings of the 9th annual ACM symposium on User interface software and technology*. 1996. ACM. DOI: http://dx.doi.org/10.1145/237091.237102
37. Richardson, Anthony E, Daniel R Montello, and Mary Hegarty, *Spatial knowledge acquisition from maps and from navigation in real and virtual environments.* Memory & cognition, 1999. **27**(4): p. 741-750. DOI: http://dx.doi.org/10.3758/BF03211566
38. Robles-De-La-Torre, Gabriel and Vincent Hayward, *Force can overcome object geometry in the perception of shape through active touch.* Nature, 2001. **412**(6845): p. 445-448. DOI: http://dx.doi.org/10.1038/35086588
39. Sanchez-Vives, Maria V and Mel Slater, *From presence to consciousness through virtual reality.* Nature Reviews Neuroscience, 2005. **6**(4): p. 332-339. DOI: http://dx.doi.org/10.1038/nrn1651
40. Satava, Richard M, *Virtual reality surgical simulator.* Surgical endoscopy, 1993. **7**(3): p. 203-205. DOI: http://dx.doi.org/10.1007/BF00594110

41. Seymour, Neal E, Anthony G Gallagher, Sanziana A Roman, Michael K O'brien, Vipin K Bansal, Dana K Andersen, and Richard M Satava, *Virtual reality training improves operating room performance: results of a randomized, double-blinded study.* Annals of surgery, 2002. **236**(4): p. 458-464, URL: https://www.ncbi.nlm.nih.gov/pmc/articles/PMC1422600/

42. Spillmann, Jonas, Stefan Tuchschmid, and Matthias Harders, *Adaptive space warping to enhance passive haptics in an arthroscopy surgical simulator.* IEEE transactions on visualization and computer graphics, 2013. **19**(4): p. 626-633. DOI: http://dx.doi.org/10.1109/TVCG.2013.23

43. Steuer, Jonathan, *Defining virtual reality: Dimensions determining telepresence.* Journal of communication, 1992. **42**(4): p. 73-93. DOI: http://dx.doi.org/10.1111/j.1460-2466.1992.tb00812.x

44. Tolani, Deepak, Ambarish Goswami, and Norman I Badler, *Real-time inverse kinematics techniques for anthropomorphic limbs.* Graphical models, 2000. **62**(5): p. 353-388.DOI: https://doi.org/10.1006/gmod.2000.0528

45. Valkov, Dimitar, Alexander Giesler, and Klaus H Hinrichs. *Imperceptible depth shifts for touch interaction with stereoscopic objects*. in *Proceedings of the SIGCHI Conference on Human Factors in Computing Systems*. 2014. ACM. DOI: http://dx.doi.org/10.1145/2556288.2557134

46. Wachs, Juan Pablo, Mathias Kölsch, Helman Stern, and Yael Edan, *Vision-based hand-gesture applications.* Communications of the ACM, 2011. **54**(2): p. 60-71. DOI: http://dx.doi.org/10.1145/1897816.1897838

47. Wiktorin, Christina, Lena Karlqvist, and Jörgen Winkel, *Validity of self-reported exposures to work postures and manual materials handling.* Scandinavian journal of work, environment & health, 1993: p. 208-214, URL: http://www.jstor.org/stable/40966137

48. Zhai, Shumin and Paul Milgram. *Quantifying coordination in multiple DOF movement and its application to evaluating 6 DOF input devices*. in *Proceedings of the SIGCHI conference on Human factors in computing systems*. 1998. ACM Press/Addison-Wesley Publishing Co. DOI: http://dx.doi.org/10.1145/274644.274689